DOI: 10.1002/eji.201948116 Eur. J. Immunol. 2020. 50: 270–2

European Journal of Immunology

Tumor immunology

Research Article

ER-aminopeptidase 1 determines the processing and presentation of an immunotherapy-relevant melanoma epitope

Kathrin Textoris-Taube[*1], *Clemens Cammann*[*2], *Petra Henklein*[3], *Eylin Topfstedt*[2], *Frédéric Ebstein*[3], *Sarah Henze*[4], *Juliane Liepe*[4], *Fang Zhao*[5], *Dirk Schadendorf*[5], *Burkhardt Dahlmann*[3], *Wolfgang Uckert*[6], *Annette Paschen*[5], *Michele Mishto*[7,8] *and Ulrike Seifert*[2]

[1] Shared Facility for Mass Spectrometry, Berlin Institute of Health, Institut für Biochemie, Charité-Universitätsmedizin Berlin, Corporate Member of Freie Universität Berlin, Humboldt-Universität zu Berlin, Berlin, Germany
[2] Friedrich Loeffler Institut für Medizinische Mikrobiologie-Virologie, Universitätsmedizin Greifswald, Greifswald, Germany
[3] Berlin Institute of Health, Institut für Biochemie, Charité-Universitätsmedizin Berlin, Corporate Member of Freie Universität Berlin, Humboldt-Universität zu Berlin, Berlin, Germany
[4] Max Planck Institute for Biophysical Chemistry, Göttingen, Germany
[5] Klinik für Dermatologie, Universitätsklinikum Essen, Essen and German Cancer Consortium (DKTK), Universität Duisburg-Essen, Essen, Germany
[6] Max-Delbrück-Centrum für Molekulare Medizin in der Helmholtz Gemeinschaft, Berlin, Germany
[7] Centre for Inflammation Biology and Cancer Immunology (CIBCI) & Peter Gorer Department of Immunobiology, King's College London, London, United Kingdom
[8] Centro Interdipartimentale di Ricerca sul Cancro "Giorgio Prodi", University of Bologna, Bologna, Italy

Dissecting the different steps of the processing and presentation of tumor-associated antigens is a key aspect of immunotherapies enabling to tackle the immune response evasion attempts of cancer cells. The immunodominant glycoprotein gp100$_{209\text{-}217}$ epitope, which is liberated from the melanoma differentiation antigen gp100^{PMEL17}, is part of immunotherapy trials. By analyzing different human melanoma cell lines, we here demonstrate that a pool of N-terminal extended peptides sharing the common minimal epitope is generated by melanoma proteasome subtypes. In vitro and in cellulo experiments indicate that ER-resident aminopeptidase 1 (ERAP1)—but not ERAP2—defines the processing of this peptide pool thereby modulating the T-cell recognition of melanoma cells. By combining the outcomes of our studies and others, we can sketch the

Correspondence: Prof. Ulrike Seifert
e-mail: ulrike.seifert@med.uni-greifswald.de

*Joint first authors.

complex processing and endogenous presentation pathway of the gp100$_{209\text{-}217}$-containing epitope/peptides, which are produced by proteasomes and are translocated to the vesicular compartment through different pathways, where the precursor peptides that reach the endoplasmic reticulum are further processed by ERAP1. The latter step enhances the activation of epitope-specific T lymphocytes, which might be a target to improve the efficiency of anti-melanoma immunotherapy.

Keywords: CD8$^+$ T cells · proteasome · ER-aminopeptidase · melanoma · gp100

Additional supporting information may be found online in the Supporting Information section at the end of the article.

Introduction

Recognition and destruction of malignant cells by CD8$^+$ cytotoxic T lymphocytes (CTLs) are the underlying mechanisms of the three leading approaches in cancer immunotherapy. At first, injection of antibodies blocking the immune checkpoints CTLA-4 or PD-1, which causes activation of patient's T cells, has emerged as a breakthrough in antitumor therapy. Secondly and thirdly, adoptive transfer of tumor-specific CTLs and therapeutic vaccination are under preclinical as well as clinical investigation. A key factor in these latter immunotherapies is the selection of optimal epitopes that are presented by major histocompatibility complex (MHC) class I molecules to CTLs [1–3].

Tumor-expressed T cell epitopes are generated, transported, and presented at the cell surface by MHC class I molecules via the antigen processing and presentation pathway (APP). The majority of these epitopes are produced by proteasome complexes, which are the central proteolytic unities of the ubiquitin-proteasome-system. Proteasomes generate MHC class I-restricted epitopes by canonical peptide-bond hydrolysis as well as by post-translational peptide splicing [4]. The proteasome's 20S catalytic core particle is arranged as four staggered rings, each containing seven non-identical subunits. The outer rings contain the α subunits (α1–α7), which form the 'gates' through which substrates enter and products are released. Each of the two inner rings contains the β subunits (β1–β7), three of which (β1, β2, and β5) harbor the six active sites. In some hematopoietic cell types and in the presence of type I and/or type II interferons, the β1, β2, and β5 standard subunits are replaced by their alternative variants, the immunosubunits β1i/LMP2 (low molecular weight protein), β2i/MECL-1 (multicatalytic endopeptidase complex like 1), and β5i/LMP7, thereby forming de-novo synthesized immunoproteasomes [5, 6]. Besides standard- and immunoproteasome complexes, expression of intermediate- or mixed-type proteasomes containing both standard- and immunoproteasome subunits have been detected in various tumor cells as well as in healthy tissue [7–9]. These proteasome isoforms quantitatively differ in their capability to produce peptides although the existence of proteasome-specific substrate cleavage sites and peptide products is still a matter of discussion [7, 8, 10–15].

Following generation by proteasomes, the epitopes and their precursor-peptides can be destroyed or further processed in the cytosol by aminopeptidases such as tripeptidyl peptidase 2 (TPP2) [16]. Peptides that survive this APP step are often translocated into the ER lumen via TAP, where peptides can be further trimmed by the IFN-γ inducible ER-resident aminopeptidases ERAP1 and/or ERAP2 [17, 18]. In addition, ERAP1/2 has been shown to be constitutively expressed in different tissues and tumor cells, where the ERAP1 level correlated with MHC class I expression [19–21]. Whereas the generation of various, mainly viral, epitopes is enhanced by ERAP1 [22], some tumor epitopes are destroyed by ERAP1 activity [23, 24], thereby suggesting that N-terminal trimming in the ER can be a key step of MHC class I antigen presentation and recognition of both infected and cancer cells [25]. So far, no precise role of ERAP2 in MHC class I epitope generation could be defined, although its specificity has been characterized to be distinct from ERAP1 activity [18, 26]. In general, the specific mechanism of ERAP1 and/or ERAP2 function could not be clarified so far. Although ERAP1 and ERAP2 have been shown to trim peptides in solution separately and also completing each other's activity, ERAP1/2 heterodimer formation has been proposed to exist in cells. However, the exact nature of the in vivo heterodimer could not be demonstrated so far. An artificially created ERAP1-ERAP2 heterodimer was shown to change the enzymatic parameters of ERAP1 leading to increased peptide trimming efficacy of the ERAP1/2 complex in vitro [27]. Furthermore, ERAP1-ERAP2 heterodimer constructs have been shown to trim precursor peptides while they are bound to MHC class I molecules, albeit no direct ERAP/MHC interaction could be detected [28]. Peptides are further handled by the peptide loading complex, which inserts the peptide into the binding groove of the MHC class I molecules according to their sequence affinity [29, 30].

Initially identified by the Rosenberg lab, the melanoma-associated glycoprotein 100 (gp100)$_{209\text{-}217}$ epitope has been frequently targeted in clinical anti-melanoma trials, mainly in its anchor-modified form (gp100$_{209\text{-}217/(T210M)}$) to enhance HLA-A*02:01 binding affinity [31–34]. The T210M substitution not only improves the binding of the gp100$_{209\text{-}217/T210M}$ epitope to HLA-A*02:01 but also alters significantly the proteasomal processing of that antigenic sequence [35]. The gp100$_{209\text{-}217}$ epitope

is derived from the melanocyte differentiation protein gp100 (also called PMEL or Pmel17), which belongs to the group of differentiation antigens expressed by tumor cells and healthy tissue of origin. PMEL can be frequently detected in metastatic melanomas making it a suitable target for cancer immunotherapy [36].

The $gp100_{209\text{-}217/T210M}$ epitope can be recognized by CTLs not only in its minimal version but also in its N-terminal extended versions $gp100_{207\text{-}217/T210M}$ and $gp100_{208\text{-}217/T210M}$. The latter peptides bind the HLA-A*02:01 complex with lower affinity than the $gp100_{209\text{-}217/T210M}$ epitope. Any N-extended version of $gp100_{209\text{-}217}$ (from $gp100_{205\text{-}217}$ to $gp100_{208\text{-}217}$) produced by proteasomes can be trimmed in vitro by ERAP1 to the length of the minimal $gp100_{209\text{-}217}$ epitope, whereas further degradation seems to be prevented [35]. According to these results, ERAP-mediated trimming of this pool of peptides in melanoma cells should determine the CTL response and therefore affect the efficacy of immunotherapies targeting this epitope.

To test this hypothesis, we investigated in vitro and in cellulo how ERAP1 and ERAP2 control the activation of the $gp100_{209\text{-}217/(T210M)}$-specific CTL clone, which recognizes both WT $gp100_{209\text{-}217}$ and mutant $gp100_{209\text{-}217/(T210M)}$ epitopes. The experimental outcomes provided the missing information to construct the APP model of this critical melanoma antigen.

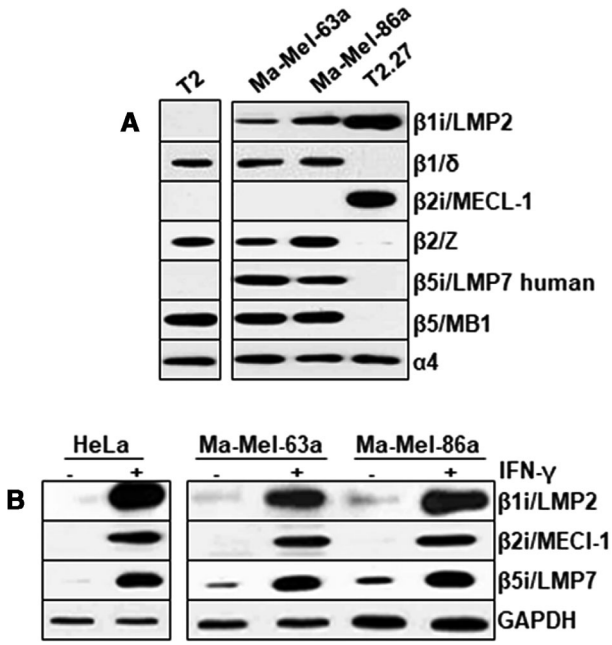

Figure 1. Proteasome content in human melanoma cell lines. (A) Subunit composition of proteasome complexes purified from the cell lines Ma-Mel-63a and Ma-Mel-86a analyzed by immunoblotting using antibodies against the indicated proteasome subunits (two technical replicates, single representative experiment). T2 cells (deficient for β1i/LMP2 and β5i/LMP7) and T2.27 cells—expressing murine β1i/LMP2, β5i/LMP7, as well as human β2/Z—were used as control and α4 served as loading control. (B) Induction of immunoproteasome subunits in Ma-Mel-63a and Ma-Mel-86a cells upon IFN-γ treatment analyzed by immunoblotting using antibodies, as indicated. Melanoma cells were exposed to 200 U/mL IFN-γ for 48 h and compared to HeLa cells (two biological replicates, one out of two independent experiments is shown). GAPDH served as loading control.

Results

Cleavage preferences of proteasome subtypes expressed in human melanoma cell lines

Since the generation and presentation of the pool of $gp100_{209\text{-}217}$-containing peptides is influenced by the proteasome isoform content of the cell [10, 12, 13, 35], we investigated the proteasome catalytic-subunit composition in two human melanoma cell lines, i.e. the gp100-expressing Ma-Mel-63a cells and the gp100-negative Ma-Mel-86a cells (Supporting Information Fig. 1A). Both melanoma cell lines expressed a mixed population of proteasome isoforms including what we inferred being the intermediate-type proteasome carrying the β1/delta, β5i/LMP7, and β2/Z or the β1i/LMP2, β5i/LMP7, and β2/Z subunits (Fig. 1A). Accordingly, analysis of purified proteasomes by two-dimensional gel electrophoresis revealed the assembly of intermediate-type proteasomes containing the two immunosubunits ß1i/LMP2 and ß5i/LMP7 in the absence of ß2i/MECL-1 (Supporting Information Fig. 1B). However, compared to isolated human spleen, ß1i and ß5i expression was considerably less pronounced in both melanoma cell lines. Based on these observations, we conclude that the melanoma cell lines Ma-Mel-63a and Ma-Mel-86a express intermediate-type proteasomes containing ß1i/LMP2, ß5i/LMP7 and ß2/Z.

Exposure of melanoma cell lines to INF-γ, which could be a frequent situation in the tumor and microenvironment, resulted in the up-regulation of all three immunosubunits including the β2i/MECL-1 subunit (Fig. 1B), thereby suggesting that the modification of the proteasome isoform content is modifiable in these cell lines.

To investigate the specific proteolytic activity of melanoma-derived 20S proteasomes we performed in vitro processing experiments of the synthetic peptide $gp100_{201\text{-}230}$ using 20S proteasomes purified from the two melanoma cell lines. The substrate and peptide products were measured by mass spectrometry (MS) and the MS outcomes were analyzed by the quantification with minimal effort (QME) method, which allowed to quantify the amount of each peptide product and to compute the substrate cleavage-site usage, i.e. the substrate site-specific cleavage strength (SCS) [37]. Correlation between in vitro experiments carried out with purified 20S proteasomes and in cellulo and in vivo experiments has been demonstrated in various studies [7, 8, 12, 13, 38–47]. Proteasomes were purified from cell lines grown in the absence of inflammatory stimuli to analyze their baseline activity. Consistently with previous studies [10, 12, 13, 35], the minimal $gp100_{209\text{-}217}$ epitope was not detectable in melanoma proteasome digestions, whereas its N-terminal extended versions could be quantified (Fig. 2A). In terms of substrate degradation and preferences of cleavage within the synthetic $gp100_{201\text{-}230}$ peptide, the proteasomes purified from the two melanoma cell lines showed a similar degradation rate and a similar cleavage pattern, which differed from that

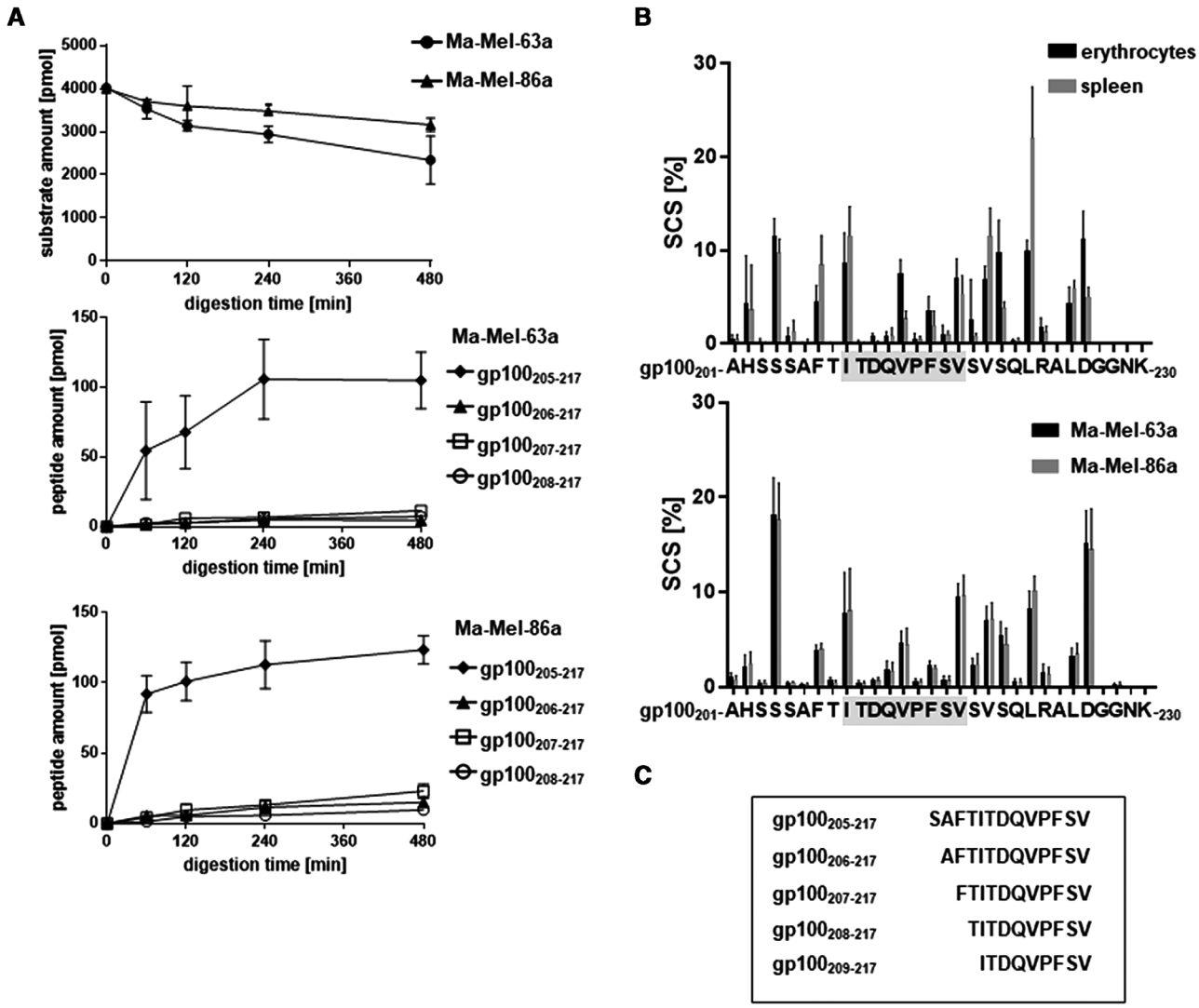

Figure 2. Gp100-related activity of 20S proteasomes isolated from different human cell lines and tissues. (A) Absolute amount of the synthetic substrate $gp100_{201-230}$ and of the $gp100_{209-217}$-containing peptides in the in vitro kinetic assays with 20S proteasome purified from Ma-Mel-63a and Ma-Mel-86a cell lines. The absolute amount of the peptide products was computed by quantification with minimal effort (QME). Values represent the mean and lines the SD of two independent experiments and two to three technical replicates. (B) Relative frequency of cleavage (SCS) after each substrate residue of the synthetic substrate $gp100_{201-230}$ by 20S proteasomes purified from Ma-Mel-63a and Ma-Mel-86a cell lines as well as from human erythrocytes and spleen. SCS was computed by QME from the in vitro kinetic assays measured by MS. Values represent the mean and lines the SD of two independent experiments and two or three technical replicates for the melanoma proteasome and two technical replicates for the human erythrocytes and spleen. (C) Scheme of the applied substrates and detected peptides throughout the study.

of proteasomes purified from human erythrocytes (standard proteasome) and spleen (immunoproteasome-enriched) (Fig. 2A and B). 20S melanoma proteasomes produced the $gp100_{205-217}$ peptide in considerably larger amounts than the shorter N-extended versions of the $gp100_{209-217}$ epitope (Fig. 2A and C). This was mediated by a strong cut between S_{204} and S_{205} at the $gp100_{205-217}$ N-terminus (Fig. 2B). All substrate cleavage sites used by erythrocyte and spleen proteasomes were used also by melanoma proteasomes, thereby confirming the hypothesis that proteasome isoforms largely cleave after the same residues although with significant quantitative differences [10, 37]. The SCSs of erythrocyte and spleen proteasomes were similar to those of a previous study carried out with 20S proteasome purified from these specimens [10], thereby confirming the robustness of this type of assay and analysis.

ERAP1 provokes degradation of the $gp100_{205-217}$ substrate as well as $gp100_{209-217}$ epitope generation

As already anticipated, 20S proteasomes obtained from melanoma cell lines did not produce the minimal $gp100_{209-217}$ epitope in detectable amounts, confirming the result of previous studies carried out with various proteasomes and conditions [10, 12, 13, 35].

Table 1. Kcat/KM of the trimming of N-extended versions of the minimal $gp100_{209-217}$ epitope by recombinant ERAP1. The Michaelis–Menten constants were computed from the in vitro digestions of the 50 μM synthetic peptides $gp100_{205-217}$, $gp100_{206-217}$, $gp100_{207-217}$, $gp100_{208-217}$, $gp100_{209-217}$ by 2.5 ng recombinant ERAP1 over time. The MS-measured results of the digestions were published previously [35]. Means and standard deviations of two independent experiments are shown. Kinetic parameters were estimated in a Bayesian framework resulting in parameter distributions and therefore providing confidence estimates (see also Supporting Information Fig. 2)

Substrate	kcat/KM [mM^{-1} min^{-1}]
$gp100_{209-217}$	1.50 ± 1.51
$gp100_{208-217}$	17.68 ± 1.99
$gp100_{207-217}$	14.12 ± 2.11
$gp100_{206-217}$	37.72 ± 5.15
$gp100_{205-217}$	17.37 ± 2.91

Two N-extended versions – *i.e.* $gp100_{208-217}$ and $gp100_{207-217}$ - have been shown to induce CTL activation *in vitro* [35]. They are produced in significant smaller amounts than the $gp100_{205-217}$ peptide by 20S proteasome purified from melanoma cell lines (Fig. 2A) and other cell types [35], though. These quantitative observations suggest that the trimming of the N-extended versions of the minimal $gp100_{209-217}$ epitope could play a significant role in the presentation of the $gp100_{209-217}$ epitope by melanoma cells to CTLs. Therefore, we computed the *in vitro* efficiency in trimming N-extended versions of the minimal $gp100_{209-217}$ epitope by recombinant ERAP1. To this end we made use of a mathematical model of ERAP1 activity and inferred the kinetic parameters based on the quantitative substrate degradation measurements of the digestions of the $gp100_{205-217}$, $gp100_{206-217}$, $gp100_{207-217}$, $gp100_{208-217}$, and $gp100_{209-217}$ synthetic peptides previously published [35] (Supporting Information Fig. 2A). The degradation kinetics of the substrates recapitulated a Michaelis–Menten-like reaction. Thus, we set out to estimate the Michaelis–Menten parameters kcat, KM, and kcat/KM (Supporting Information Fig. 2B), and reported the kcat/KM values (Table 1), which gave the best confidence in our model. The estimated kcat/KM value of $gp100_{209-217}$ peptide was significantly lower compared to the parameters of the N-extended versions, thereby reflecting the fact that the epitope was not trimmed by ERAP1 in those conditions. The ERAP1-mediated trimming efficiency for the substrates $gp100_{208-217}$, $gp100_{207-217}$, and $gp100_{205-217}$ was comparable. On the contrary, the substrate $gp100_{206-217}$ was processed with highest efficiency, most likely due to a higher kcat (Table 1 and Supporting Information Fig. 2B).

Since the $gp100_{205-217}$ peptide is generated in high amounts by the proteasome of the melanoma cell lines (Fig. 2A), we further investigated the ERAP1/2 dynamics of $gp100_{205-217}$ processing. When this peptide is trimmed by ERAP1, the $gp100_{206-217}$, $gp100_{207-217}$, $gp100_{208-217}$, and $gp100_{209-217}$ peptides/epitope are generated and no shorter peptide fragments could be detected (Fig. 3A and B). When we used very high ERAP1 enzyme concentrations (2 μg/mL) a barely detectable $gp100_{210-217}$ peptide product was measured (Supporting Information Fig. 3A). Normal concentration of ERAP2 could generate only a small

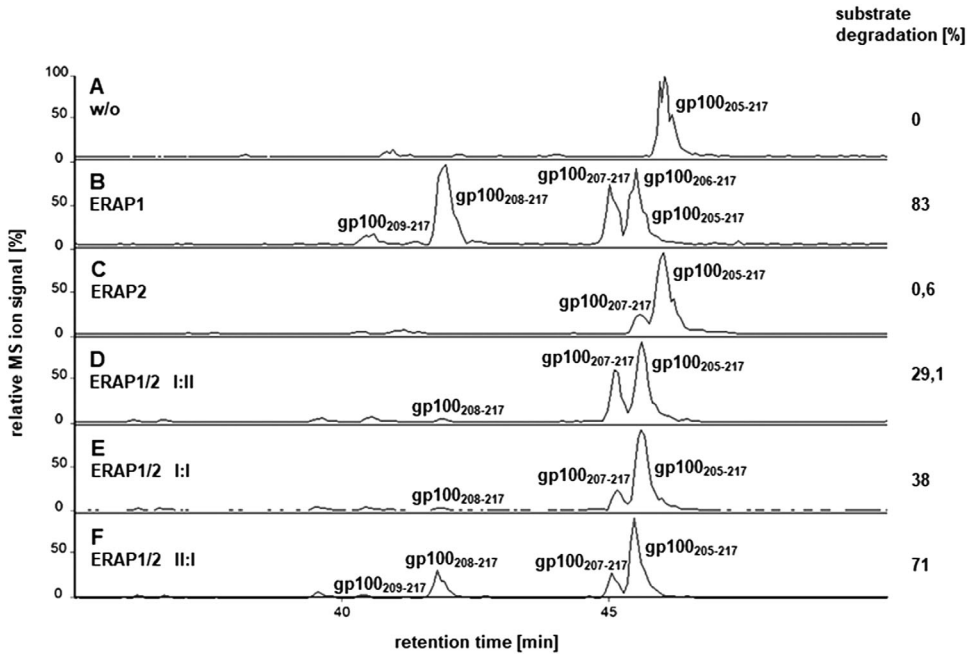

Figure 3. ERAP1 and ERAP2 trimming activity of the synthetic substrate $gp100_{205-217}$. (A–F) The epitope precursor peptide $gp100_{205-217}$ was digested in vitro for 4 h by ERAP1 and/or ERAP2 and the generated peptide fragments were measured by LC–MS. The HPLC-profiles are zoomed from 35 to 50 min. Addition of enzymes as follows: (A) substrate $gp100_{205-217}$ control, (B) ERAP1 (3 ng), (C) ERAP2 (3 ng), (D) ERAP1/2 ratio I:II (1 ng ERAP1/2 ng ERAP2), (E) ERAP1/2 ratio I:I (1.5 ng ERAP1/1.5 ng ERAP2), and (F) ERAP1/2 ratio II:I (2 ng ERAP1/1 ng ERAP2). The relative MS ion signal of the peptides $gp100_{209-217}$ (9mer epitope), $gp100_{208-217}$ (10mer), $gp100_{207-217}$ (11mer), and $gp100_{206-217}$ (12mer), which were identified by LC–MS/MS, is indicated. One out of two independent experiments is displayed.

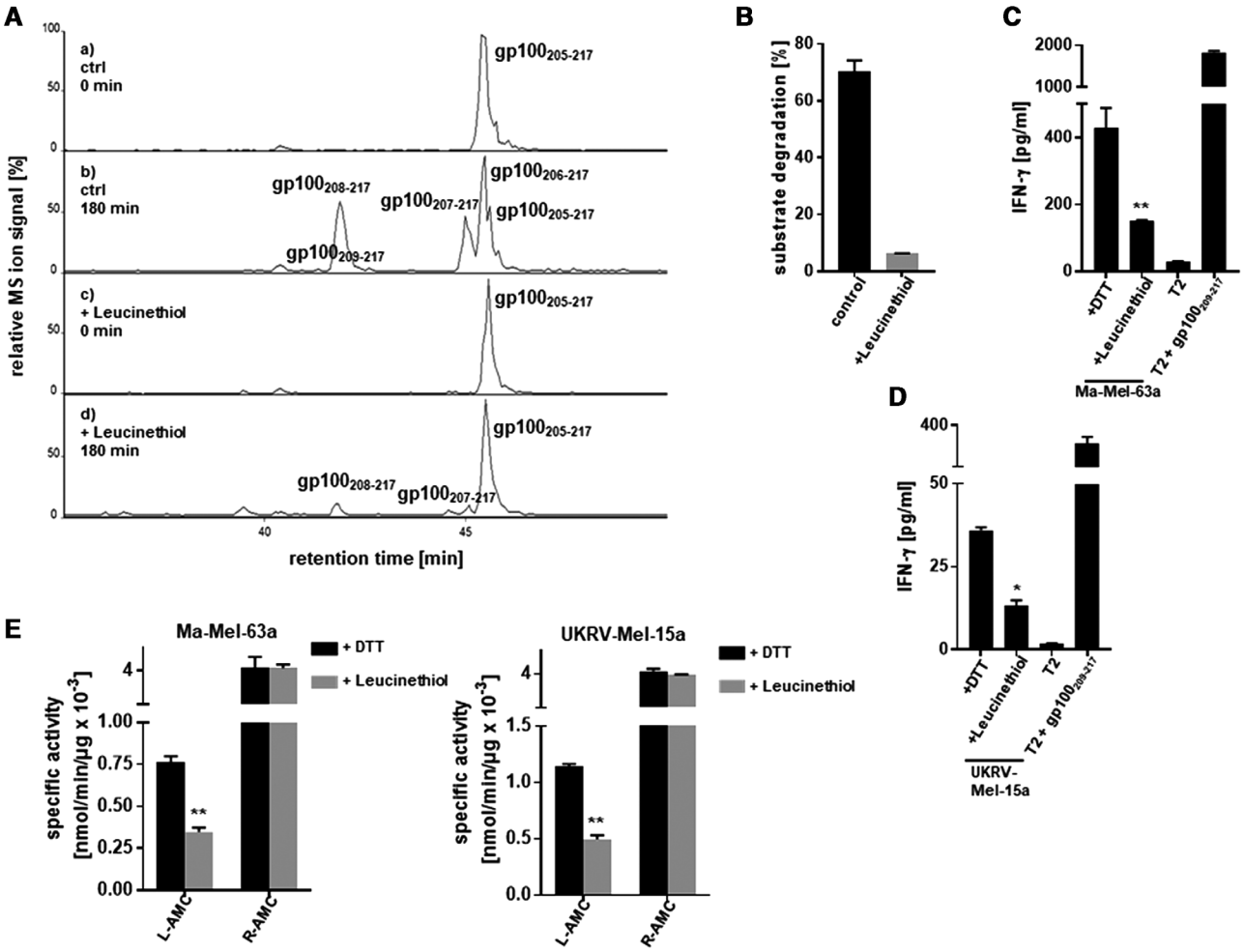

Figure 4. Endogenous $gp100_{209\text{-}217}$ epitope generation is inhibited by leucinethiol. (A) LC–MS profiles of in vitro substrate degradation of the 13mer $gp100_{205\text{-}217}$ precursor peptide by ERAP1 without and with inhibitor leucinethiol after 180 min incubation and (B) corresponding relative substrate degradation. SD (of mean) of duplicate determinations is shown as representative data from two independent experiments. (C) Ma-Mel-63a and (D) UKRV-Mel-15a cells were exposed to 30 µM leucinethiol for 16 h or to DTT as solvent control and were co-incubated with $gp100_{209\text{-}217}$-specific T lymphocytes for 16 h. IFN-γ release by gp100-specific CTLs was measured by IFN-γ ELISA. T2 cells without and with $gp100_{209\text{-}217}$ peptide were used as control for T cell specificity. Data are displayed as mean + SD of three technical replicates. One independent experiment out of two is shown (Student's t-test; $^{*}p < 0.05$; $^{**}p < 0.01$). (E) Specific activity of ERAPs in cell lysates of leucinethiol treated Ma-Mel-63a and UKRV-Mel-15a cells. Specific activity was measured through incubation of the cell lysates with the H-Leu-AMC- or the H-Arg-AMC-substrate, which display ERAP1 and ERAP2 activity, respectively. DTT-treated cells served as control. Data are displayed as mean and SD of two technical replicates (one out of two independent experiments).

amount of the $gp100_{207\text{-}217}$ epitope (Fig. 3A and C), which could be enhanced by using high ERAP2 enzyme concentrations (Supporting Information Fig. 3B and C). No smaller peptide products could be clearly identified when we used the synthetic peptides $gp100_{207\text{-}217}$, $gp100_{208\text{-}217}$, and $gp100_{209\text{-}217}$ as substrates (Supporting Information Fig. 3B and C and data not shown). This limited trimming activity of ERAP2 is substrate specific since the cleavage of the HIV-$gp160_{313\text{-}327}$ precursor peptide was efficiently carried out as expected (Supporting Information Fig. 4A and B) [17]. In ERAP1/2 digestions, the $gp100_{205\text{-}217}$ substrate degradation rate directly correlated with the ERAP1:ERAP2 relative ratio. Accordingly, more products were detectable by increasing the ERAP1:ERAP2 ratio, although in those assays where ERAP2 was present, the $gp100_{206\text{-}217}$ peptide product could not be identified (Fig. 3A–F).

To further test our hypothesis that ERAP1 promotes the generation of immunogenic $gp100_{209\text{-}217}$-containing epitopes, we performed in vitro and in cellulo experiments by using the metalloprotease inhibitor leucinethiol, which targets ERAP1. Consistently, addition of leucinethiol to the in vitro digestion resulted in a blockade of $gp100_{205\text{-}217}$ degradation and stabilization of the precursor peptide (Fig. 4A and B). Furthermore, activation of a $gp100_{209\text{-}217}$-specific CTL clone was significantly reduced by ERAP1 inhibition in Ma-Mel-63a (Fig. 4C) and UKRV-Mel-15a melanoma cells (Fig. 4D), which both express the gp100 antigen and HLA-A*02:01. As activity control, the ability of leucinethiol

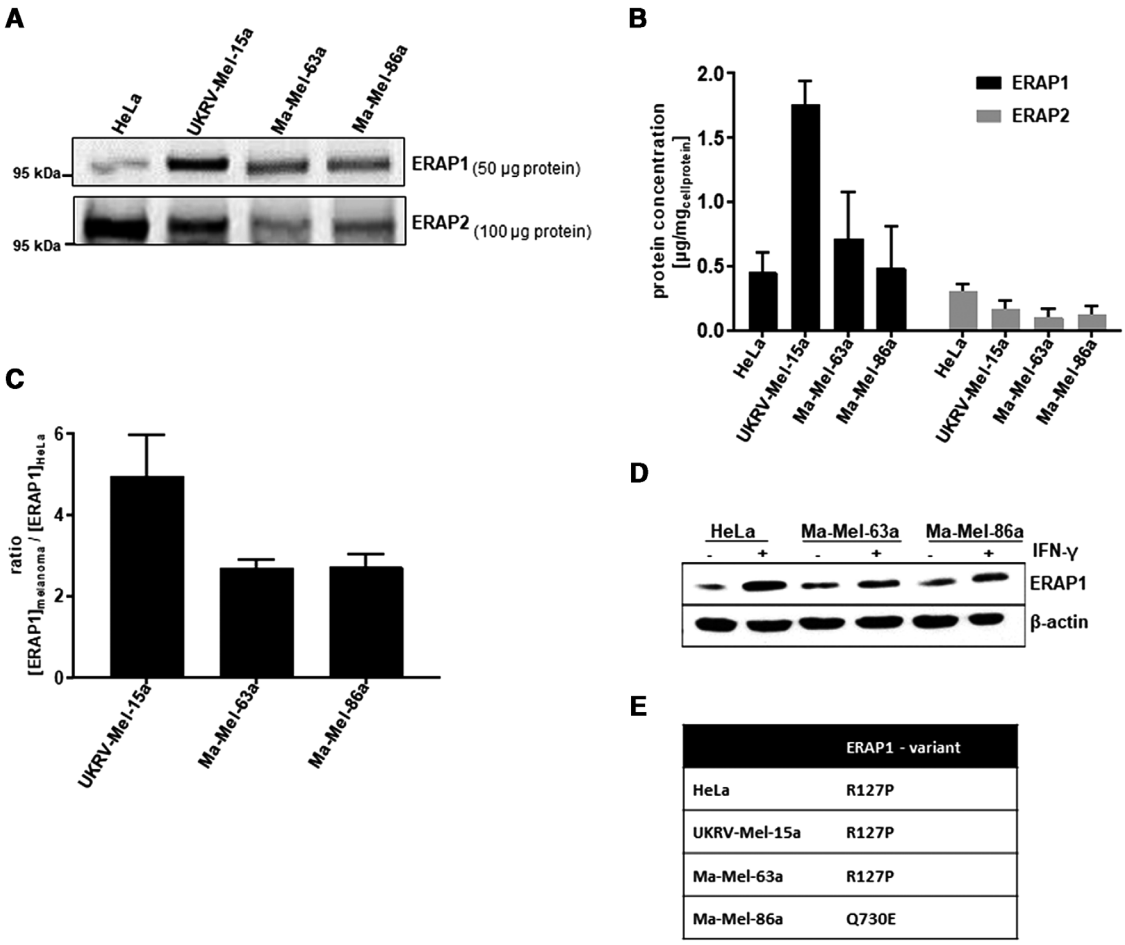

Figure 5. Quantification of ERAP1 and ERAP2 in different melanoma cell lines compared to HeLa cells. (A and B) absolute quantification of ERAP1 (50 µg protein loaded) and ERAP2 (100 µg protein loaded) concentration analyzed by western blot in HeLa, UKRV-Mel-15a, Ma-Mel-63a, and Ma-Mel-86a cells using different concentrations of recombinant ERAP1 or ERAP2 as standard. In (B) the protein band densities from independent western blot assays for ERAP1 ($n = 4$) and ERAP2 ($n = 3$) has been measured and mean + SD are shown. (C) Ratios of the ERAP1 content were analyzed by MS label-free quantification (LFQ) (UKRV-Mel-15a/HeLa cells; Ma-Mel-63a/HeLa cells; Ma-Mel-86a/HeLa cells) (mean + SD, two biological replicates measured three times). (D) ERAP1 protein expression analyzed by immunoblotting in Ma-Mel-63a and Ma-Mel-86a cells upon IFN-γ treatment (200 U/mL IFN-γ for 48 h). HeLa cells were used as control and β-actin as loading control. One out of two independent experiments is shown. (E) Allelic variants of ERAP1 were analyzed by sequencing of cloned full length ERAP1 constructs derived from total RNA of HeLa^{A2+} cells, Ma-Mel-63a, Ma-Mel-86a, and UKRV-Mel-15a cells. Previously described allelic variants found in five out of five independent clones (2/2 for HeLa^{A2+} cells) are depicted.

treated cell lysates to trim the H-Leu-AMC or the H-Arg-AMC substrate was analyzed. As expected, the turnover of the H-Leu-AMC—representing ERAP1 activity—was significantly reduced in the presence of leucinethiol, whereas the H-Arg-AMC substrate—representing ERAP2 activity—was not affected (Fig. 4E).

ERAP1, but not ERAP2, promotes activation of gp100$_{209\text{-}217}$-specific CTL clones by melanoma cell lines

These results suggested a beneficial impact of ERAP1 rather than ERAP2 in defining the presentation of the gp100$_{209\text{-}217}$-containing peptides/epitope by melanoma cells to CTLs. We tested this hypothesis and the ERAP1/2 content in human melanoma cell lines Ma-Mel-63a, Ma-Mel-86a, and UKRV-Mel-15a. They all expressed both ERAP1 and ERAP2, although ERAP2 expression was lower than ERAP1 with different ERAP1:ERAP2 ratio among the melanoma cell lines (Fig. 5A–C). Upon exposure to IFN-γ, ERAP1 expression was enhanced in both Ma-Mel-86a cells and Ma-Mel-63a cells (Fig. 5D) and also in UKRV-Mel-15a cells as shown before [24]. Since ERAP activity could be influenced by the various polymorphisms that these enzymes have, we analyzed the ERAP1 alleles present in the investigated cell lines. Amongst others, we observed two described polymorphisms associated with the risk of cancer development [48, 49]. The R127P polymorphism in HeLa, UKRV-Mel-15a and Ma-Mel-63a and the Q730E mutation in Ma-Mel-86a cells suggest an altered peptide trimming activity in the latter [50] (Fig. 5E).

To test whether ERAP1 and ERAP2 could impinge upon the presentation of the gp100$_{209\text{-}217}$-containing peptides/epitope by

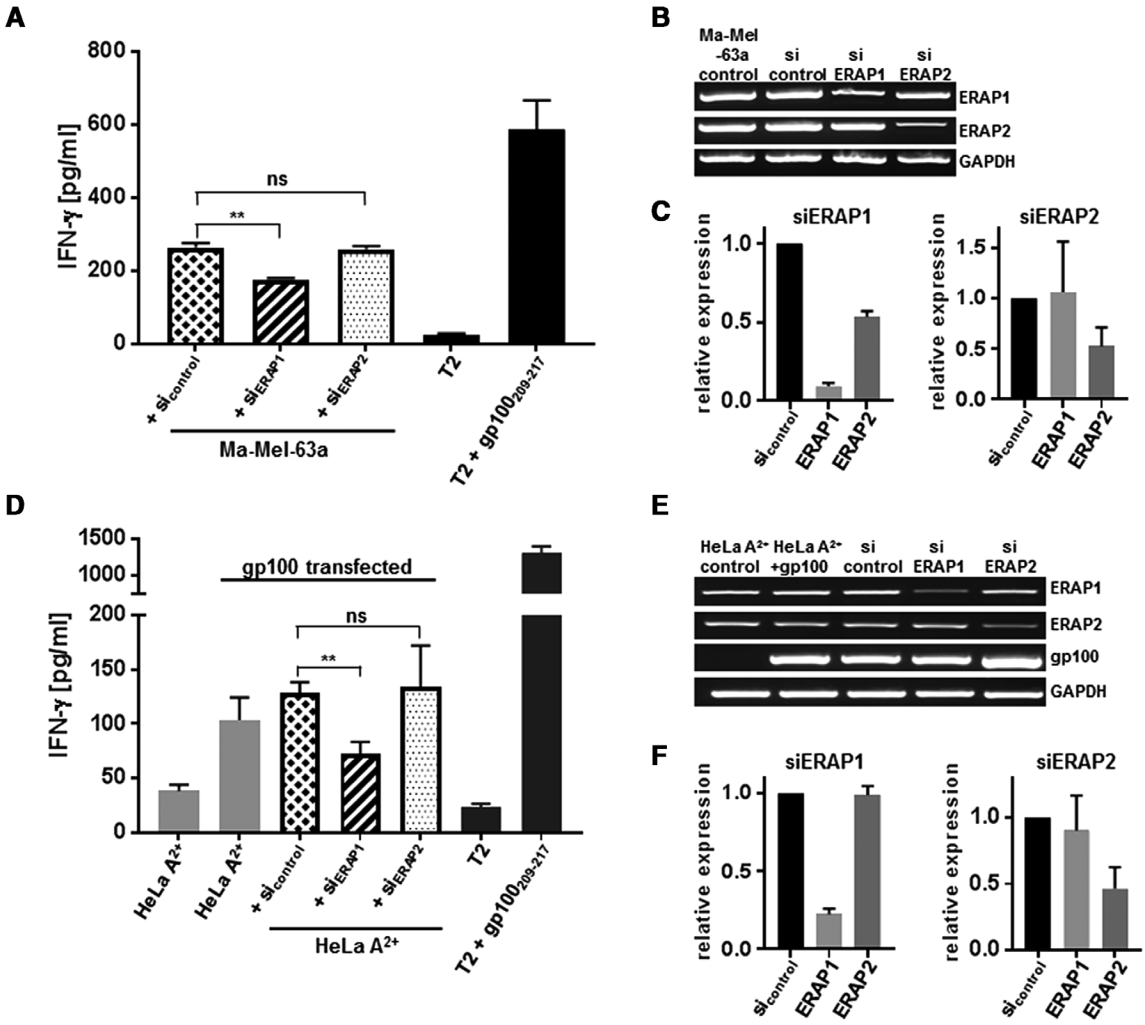

Figure 6. ERAP1 but not ERAP2 impinges upon the activation of the $gp100_{209\text{-}217}$-specific CTL clones. (A) IFN-γ-production of $gp100_{209\text{-}217}$-specific CTL clones incubated for 16 h with Ma-Mel-63a melanoma cells expressing HLA-A*02:01 and the gp100 antigen. Ma-Mel-63a cells were pretreated with 30 nM ERAP1, ERAP2, and control siRNA for 72 h. T2 cells served as negative and $gp100_{209\text{-}217}$-peptide loaded T2 cells as positive control, the mean and the SD of three technical replicates are shown. Student's *t*-test; $p < 0.01$. (B) Ma-Mel-63a cell RNA was analyzed for down-regulation of ERAP1 and ERAP2. GAPDH served as loading control. (C) qPCR analysis of ERAP1 and ERAP2 down-regulation in Ma-Mel-63a cells. Relative expression was calculated in comparison to control siRNA treated cells and 18S rRNA served as housekeeping gene. The means and SD of three technical replicates are shown. (D) IFN-γ production of $gp100_{209\text{-}217}$ specific cytotoxic T cells incubated for 16 h with gp100 transfected $HeLa^{A2+}$ cells (HeLa cells expressing HLA-A*02:01). $HeLa^{A2+}$ cells were pretreated with siRNA against ERAP1 or ERAP2 as well as control siRNA for 72 h. T2 cells served as negative and $gp100_{209\text{-}217}$-peptide loaded T2 cells as positive control, the mean and the SD of three technical replicates are represented. Student's *t*-test; $p < 0.01$. (E) HeLa cell RNA was tested for down-regulation of ERAP1 and ERAP2 and overexpression of gp100. GAPDH served as loading control. (F) qPCR analysis of ERAP1 and ERAP2 down-regulation in $HeLa^{A2+}$ cells. Relative expression was calculated in comparison to control siRNA treated cells and 18S rRNA served as housekeeping gene. The mean and SD of three technical replicates are shown. One out of two independent experiments is shown (A–F).

melanoma cell lines to CTLs, we performed siRNA knock down of either ERAP1 or ERAP2 in Ma-Mel-63a cells. In agreement with our in vitro results, knocking down ERAP1 significantly reduced the $gp100_{209\text{-}217}$-specific CTL activation, whereas silencing ERAP2 displayed no significant alterations of the amount of IFN-γ released by the CTL clone (Fig. 6A–C). Similar results were obtained when we used UKRV-Mel-15a (Supporting Information Fig. 5A and B) and gp100-transfected $HeLa^{A2+}$ (HeLa cells expressing HLA-A*02:01) cell line clones (Fig. 6D–F). This hints toward the hypothesis that ERAP1, rather than ERAP2, promotes the activation of $gp100_{209\text{-}217}$-specific CTLs by increasing the presentation of $gp100_{209\text{-}217}$ epitopes by melanoma cell lines as well as by other cancer cell lines.

Discussion

The modified $gp100_{209\text{-}217/(T210M)}$ melanoma epitope has been part of successful phase 2/3 clinical trials combining the $gp100_{209\text{-}217/(T210M)}$ peptide with interleukin-2 application [34]. However, combined administration of gp100 peptides together with the CTLA-4-antagonist ipilimumab in patients with metastatic

melanoma displayed no improvement in disease progression compared to patients treated with ipilimumab alone, thereby suggesting an insufficient presentation of the gp100$_{209\text{-}217}$ epitope at least in parts of the melanoma [51, 52].

Our results provide further information about the APP of the gp100$_{209\text{-}217}$-containing epitopes and specifically the role that ERAP1 rather than ERAP2 plays in promoting epitope presentation. Both in vitro kinetic analyses and *in cellulo* inhibitor and siRNA experiments demonstrated that ERAP1 generates and stabilizes the minimal gp100$_{209\text{-}217}$ epitope. This is in contrast to the MART-1$_{26\text{-}35}$ (melanoma antigen recognized by T cells) epitope being destroyed by ERAP1 [24]. ERAP1 has been shown to be constitutively expressed in tumor cells, even in the absence of IFN-γ [19, 24]. Analyzing three different melanoma cell lines, we found differences in ERAP1 expression (Fig. 5). We could detect two ERAP1 polymorphisms (R127P and Q730E), which are correlated with an increased risk of cancer development [49, 53]. However, only the Q730E mutation has been shown to display reduced peptide trimming activity suggesting an impaired gp100$_{209\text{-}217}$ epitope generation in melanoma cells expressing the Q730E variant [50]. To note, we did not observe any effect of ERAP2 on gp100$_{209\text{-}217}$ epitope processing, neither in in vitro digestions—using ERAP2 alone or in combination with ERAP1—nor in cellular antigen presentation assays analyzing ERAP1/2 activity based on ERAP natural expression in melanoma cells.

By combining the outcome of this and other studies [12, 13, 35, 54], we can sketch how gp100$_{209\text{-}217}$-containing epitopes are presented to CTLs: in the cytosol, proteasomes produce two potential epitopes, i.e. gp100$_{207\text{-}217/T210M}$ and gp100$_{208\text{-}217/T210M}$ that share the gp100$_{209\text{-}217/T210M}$ minimal sequence I**T**/**M**DQVPFSV. The WT gp100$_{207\text{-}217}$ and gp100$_{208\text{-}217}$ peptides bind with low affinity to the HLA-A*02:01 complex, therefore their in vivo immunogenicity is disputable, and these are most likely only sources for the gp100$_{209\text{-}217}$ generation in the ER. In contrast, the T210M gp100$_{207\text{-}217}$ and gp100$_{208\text{-}217}$ peptides bind to the HLA-A*02:01 complex with higher affinity and trigger a stronger CTL response in vitro than the WT gp100$_{209\text{-}217}$ epitope [35]. Furthermore, melanoma proteasomes, which contain intermediate-type proteasomes, as shown for both Ma-Mel-63a and Ma-Mel-86a cells here as well as in previously published literature [7, 13], abundantly generate the N-extended version of the gp100$_{209\text{-}217}$-epitope, i.e. the gp100$_{205\text{-}217}$ precursor. In the cytosol, the epitopes (and likely also their N-extended precursors) can be destroyed by TPP2 [54]. The peptides that survive this step can be translocated into the ER lumen via TAPs and to the endosomal compartment by another unknown carrier. In the ER, the peptides gp100$_{205\text{-}217}$, gp100$_{206\text{-}217}$, gp100$_{207\text{-}217}$, and gp100$_{208\text{-}217}$ can be trimmed by ERAP1—but not by ERAP2—thereby augmenting the amount of the gp100$_{209\text{-}217}$-containing epitopes, as shown in the present study and in ref. [35]. For those gp100$_{209\text{-}217/T210M}$-containing epitopes that followed the canonical TAP-dependent pathway, the allocation into the HLA-A*02:01 binding groove is likely mediated by the peptide loading complex. For the portion of

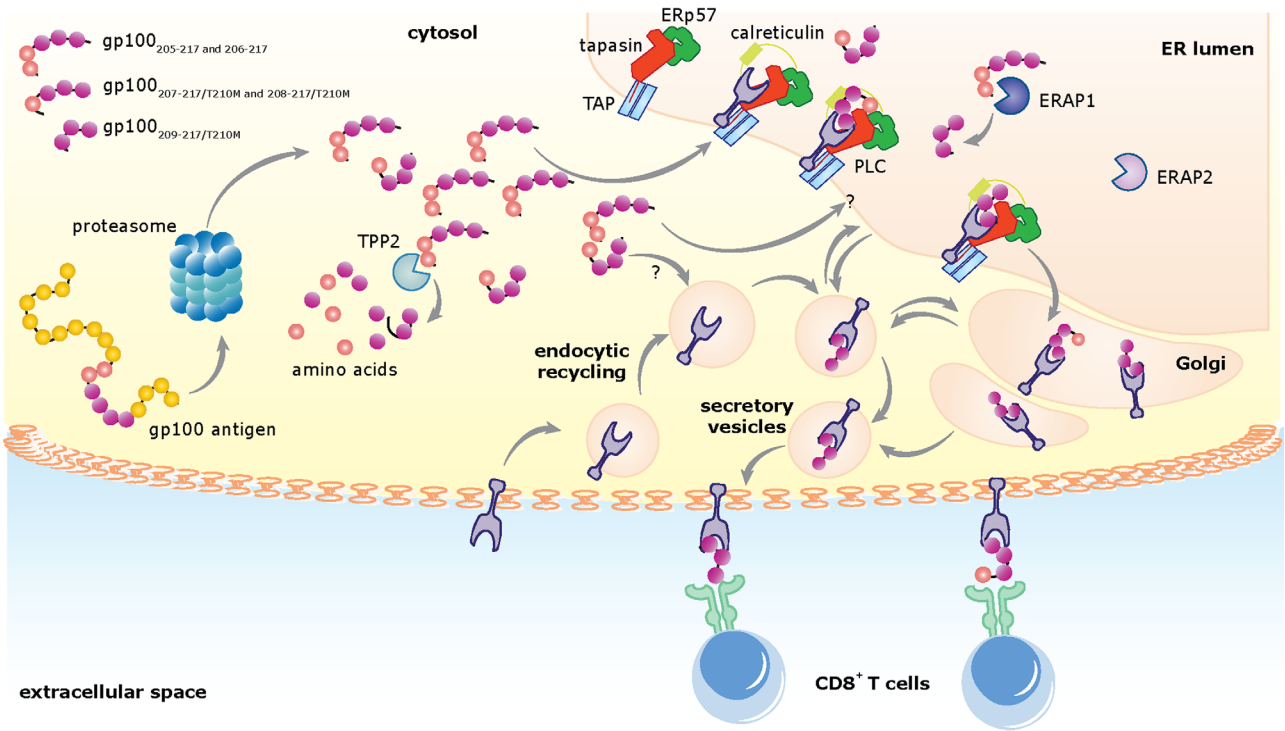

Figure 7. APP of the gp100$_{209\text{-}217/T210M}$-containing epitopes/peptides. Explanation of the pathway can be found in the discussion section. With the nomenclature gp100$_{207\text{-}217/T210M}$ and gp100$_{208\text{-}217/T210M}$ as well as gp100$_{209\text{-}217/T210M}$, we refer to both WT and T210M peptides. In detail, differences between the WT and the T210M peptides are disclosed in the Discussion section. Reproduced with permission from ref. [5].

the $gp100_{209\text{-}217}$ epitope that is translocated into the endosomal pathway via an alternative route, the function of tapasin is not mandatory to efficiently present the $gp100_{209\text{-}217}$ epitope at the cell surface [54] (Fig. 7).

The APP that triggers a response of $gp100_{209\text{-}217/T210M}$-specific CTLs is therefore branched and can be carried out with success independently of several proteins/enzymes. This supports the use of this pool of epitopes/peptides in immunotherapy because a diversified APP can be a potent tool to tackle the immune-response escape attempts implemented by cancer. For example, we can speculate that even in case that cancer compromises either TAP or tapasin, the presentation of the $gp100_{209\text{-}217/T210M}$-containing epitopes could be enhanced in melanoma by inhibiting TPP2 and/or stimulating ERAP1.

Materials and methods

Cell culture

Melanoma cell lines have been described previously [55]. Melanoma cells, HeLa cells, the TAP-deficient T2 cell line, and T2.27 cells expressing murine β1i/LMP2 and β5i/LMP7 [56] were grown in RPMI1640 (Biochrom) containing 10% FCS, 2 mM L-glutamine, and 100 U/mL penicillin/streptomycin (additives from PAA Laboratories). HeLa transfectants, expressing HLA-A*02:01 ($HeLa^{A2+}$) were grown in medium supplemented with 2 μg/mL puromycin and T2.27 cells in the presence of 0.1 mg/mL G418 [56, 57].

Immunoblotting and 2-dimensional gel electrophoresis

Western blot was performed as described [58]. Briefly, 25 μg protein of cell lysate or 100 μg for gp100 detection and 1 μg of purified 20S proteasome per lane were separated on SDS-PAGE, transferred to PVDF-membranes and were immunoblotted for proteasome subunits (all laboratory stock), β1i/LMP2 (Abcam), gp100 (Abcam), and GAPDH (Santa Cruz). For ERAP1/2 detection and quantification 50 or 100 μg protein of cell lysate were blotted and probed with ERAP1 (6H9, R&D Systems), ERAP2 (3F5, R&D Systems), and β-actin (Sigma-Aldrich). Membranes were developed with ECL (GE Healthcare). For absolute quantification of ERAP1/2 in human cell lines, the western blot signal was compared to recombinant ERAP1 (10, 50, 75, and 100 ng) or ERAP2 (5, 10, 20, and 50 ng), and was quantified using ImageJ software. ERAP content in cell lysates was calculated from the resulting standard curves.

To separate the subunits of the 20S proteasome complex, isoelectric focusing by carrier ampholytes was combined with SDS-PAGE. Proteasomes were applied to a carrier ampholyte isoelectric focusing gel. In the second dimension, proteins were loaded onto SDS-PAGE and stained with Coomassie brilliant blue G-250. Proteasome subunits could be identified based on their migration behavior in comparison to reference electrophoreses of selected proteasomes [59].

20S proteasome and recombinant ERAP1/2

20S proteasomes were purified from frozen melanoma cell lines and from human spleen and erythrocytes as described [60]. Recombinant human ERAP1 and ERAP2 were purchased from R&D Systems.

Peptides

The AHSSSAFTITDQVPFSVSVSQLRALDGGNK $gp100_{201\text{-}230}$ polypeptide as well as the $gp100_{209\text{-}217}$ 9mer ITDQVPFSV and the 10mer TITDQVPFSV, 11mer FTITDQVPFSV, 12mer AFTITDQVPFSV, 13mer SAFTITDQVPFSV derive from the human melanocytic protein $gp100^{PMEL17}$ sequence. The $HIVgp160_{313\text{-}327}$ precursor peptide containing the $gp160_{319\text{-}327}$ epitope derives from the HIV gp160 glycoprotein. All peptides were synthesized using Fmoc solid phase chemistry.

In vitro digestion of short fluorogenic peptides

To control inhibition of peptidase activity in Ma-Mel-63a and UKRV-Mel-15a cells, cells exposed to leucinethiol (solved in 0.5 mM DTT) or DTT were lysed in 50 mM Tris-HCl (pH 7.5), 50 mM NaCl, 5 mM $MgCl_2$, 0.1% TritonX, and homogenized with a Dounce homogenizer. Specific peptidase activity was determined by incubation of 3 μg cell lysate with 50 μM H-Leu-AMC or H-Arg-AMC (Bachem) in 25 mM Tris-HCL (pH 7.5), 150 mM NaCl assay buffer for 30 min at 37°C, and computed as [nmol AMC/min/μg cell lysate].

Recombinant ERAP1 and ERAP2 enzymatic activity was tested by degrading the substrates H-Leu-AMC and H-Arg-AMC for ERAP1 and ERAP2, respectively. We used various substrate concentrations (10-200 μM) and 0.1 μg ERAPs in 25mM Tris (pH 7.5). The specific activity was 0.156 nmol/min/μg (ERAP1) and 0.05 nmol/min/μg (ERAP2) and comparable to the activities described by the manufacturer (R&D systems).

The fluorescence was measured by Tecan fluorometer using excitation 360 nm and emission 460 nm wavelength in a kinetics experiment (0–20 min). The free AMC calibration curve was done by measuring the fluorescence of free AMC at various concentrations (0–1 μM).

In vitro digestion of synthetic peptide substrate by purified 20S proteasome

The synthetic peptide $gp100_{201\text{-}230}$ (40 μM) was digested by 3 μg of purified 20S proteasomes in 100 μL TEAD buffer (20 mM Tris,

1 mM EDTA, 1 mM NaN_3, 1 mM DTT, pH 7.2) in kinetic experiments (0–8 h) at 37°C. For the assays performed with melanoma proteasomes we carried out two biological replicates, each of them measured 2–3 times by MS. For the assays performed with erythrocyte and spleen proteasomes we carried out one assay, measured twice by MS since the outcome recapitulated the results described previously [10]. Liquid chromatography–mass spectrometry (LC-MS) analyses of polypeptide digestion products were performed using the ESI-ion trap instrument DECA XP MAX (ThermoFisher Scientific, USA) as previously described [61]. Database searching was performed using SpliceMet's ProteaJ, which allowed the identification of spliced and non-spliced peptide products [61]. Quantification of proteasome-generated peptides and computation of the substrate SCS was carried out by applying the QME (Quantification with Minimal Effort) method to the LC-MS analyses [37]. QME estimated the absolute content of peptide products based on their MS ion peak area measured in the digestion probe. The QME algorithm parameters were empirically computed in our previous study [37] and here applied. SCS describes the relative frequencies of proteasome cleavage after any given residue of the synthetic polypeptide substrates [37]. The SCS values shown in this study are the average of SCS measured over time [37].

Analysis of in vitro digestions of precursor peptides with ERAPs

Fifty micromolar of peptides were digested in vitro with 3 ng recombinant ERAP1 or recombinant ERAP2 in 20 μL assay buffer (25 mM Tris, pH 7.5, 150 mM NaCl, 0.5 μg/mL albumin) at 37°C. For high enzyme concentrations, 25 μM of peptides were digested with 2 μg/mL ERAP1 or ERAP2 [18]. To inhibit ERAP1 activity, 3 ng recombinant enzyme were pre-incubated with 30 μM leucinethiol at room temperature for 20 min and then applied to in vitro processing experiments. For the analysis of the digestion products obtained from the $gp100_{205\text{-}217}$ precursor peptide, different ERAP1/ERAP2 ratios (pre-incubation 30 min at room temperature) were used, total enzyme concentration (3 ng/20 μL digestion volume) and peptide concentration (50 μM) were constant, recombinant ERAP1/ERAP2 ratio is indicated in Fig. 3. The digestion period was 4 h. Experiments were performed at least twice. Peptide products were identified by LC-MS/MS, as described for in vitro proteasome experiments (see above). Substrates' abundance was quantified through the titration of synthetic peptides.

To analyze the substrate trimming dynamics of ERAP1, we applied a mathematical model describing Michaelis–Menten kinetics. We estimated the kinetic parameters of the model Km and kcat of the trimming of the synthetic substrates $gp100_{205\text{-}217}$, $gp100_{206\text{-}217}$, $gp100_{207\text{-}217}$, $gp100_{208\text{-}217}$, $gp100_{209\text{-}217}$ by purified ERAP1 in two of the kinetics experiments described elsewhere [35].

The model reactions can be depicted as follows: $S + E \leftrightarrow [SE] \rightarrow P + E$, resulting in the ordinary differential equation model describing substrate degradation over time t: $dS/dt = -E*kcat*S / (KM+S)$, where S is the substrate, P is the sum of all products, E is the enzyme ERAP1; KM is the Michaelis–Menten constant; kcat describes the trimming of the substrate to products P (also maximal velocity). According to our model, although a large range of KM and kcat values could result in a good model fit with the experimental data, the KM and kcat were strongly correlated (Supporting Information Fig. 2B). Hence, we could compute ERAP1 efficiency as the ratio kcat/KM and then derivate the parameter confidence distribution for KM and kcat (Supporting Information Fig. 2B). The parameters kcat, KM, and kcat/KM were estimated using exact Bayesian inference in a Markov Chain Monte Carlo scheme. The latter resulted in posterior parameter distributions (rather than single point estimates) and therefore we could also provide with an estimate of the parameter uncertainty. The medians and standard deviations (SD) of the marginal posterior parameter distributions are reported in Table 1.

Identification and quantification of ERAP1 in the lysates of different cell lines were performed as described before [62]. LC-MS runs were conducted as follows: samples were trapped and then analyzed by nanoscale LC-MS/MS measurements using a Q Exactive Plus mass spectrometer coupled with an Ultimate 3000 RSLCnano (ThermoFisher Scientific). Protein identification and relative label-free quantification were performed using MaxQuant software version 1.6.0.1 [62] and Andromeda label-free quantification parameters were set to default. Spectra were matched to a human database (20 244 reviewed entries, downloaded from swissprot.org), a contaminant, and decoy database. In addition, protein identifications were calculated with FDR = 1% and proteins with one razor peptide per protein were used for identification. Lysates were digested twice and analyzed three times.

T-cell stimulation

For CTL-experiments PBLs obtained from healthy donors after informed consent and Ethical Committee (Charité) approval were transduced with the $gp100_{209\text{–}217/(T210M)}$ epitope-specific T-cell receptor (recognizing the IMDQVPFSV peptide and the ITDQVPFSV peptide) [63]. In CTL assays the following target cells were used: UKRV-Mel-15a and Ma-Mel-63a cells exposed to 30 μM leucinethiol (Bachem) (solved in 0.5 mM DTT) for 16 h, $HeLa^{A2+}$, Ma-Mel-63a, UKRV-Mel-15a, and T2 cells. In order to silence ERAP1/2, $HeLa^{A2+}$ cells, Ma-Mel-63a or UKRV-Mel-15a cells were transfected with 30/100 nM siGENOME human ERAP1 siRNA-SMARTpool (#M-005787-02-0005, Dharmacon) or 30/100 nM siGENOME human ERAP2 siRNA-SMARTpool (#M-005934-02-0005, Dharmacon) for 72 h. As control, 30/100 nM non-targeting siRNA (#D-001206-13-05, Dharmacon) was employed. $HeLa^{A2+}$ cells were transiently transfected with 3 μg of an expression plasmid encoding $gp100^{PMEL17}$ (pcDNA3.1/myc-HIS/gp100mel [40]) for 24 h according to the manufacturer's instructions (Lipofectamine 2000, Invitrogen), followed by co-incubation of target cells and $gp100_{209\text{–}217/T210M}$ specific T lymphocytes for 16 h, IFN-γ-release in the supernatants was determined by human IFN-γ ELISA Kit (Biolegend). Co-incubation with T2 cells served as negative control, whereas T2 cells loaded with 1 μg/mL $gp100_{209\text{-}217}$

peptide for 16 h were used as positive control. T cell assays presented in this work were performed compliant to MIATA guidelines.

Confirmation of siRNA knock down by RT-PCR

Total RNA from HeLa^{A2+} cells, Ma-Mel-63a and UKRV-Mel-15a cells was isolated using the Trizol reagent (Thermo Fisher Scientific). Reverse transcription was performed with M-MLV Reverse Transcriptase (Promega). Expression of ERAP1/2 was analyzed by RT-PCR and qPCR. GAPDH and gp100 were used as controls. RT-PCR primers were used as indicated: ERAP1 forward 5′-CC ACTCCTTCATGGTGTCAG-3′ and reverse 5′-GCAACAGTCAC AGATTTCAC-3′; ERAP2 forward 5′-CTGCTTAACAGCCATCTTGC-3′ and reverse 5′-CATCACCTAACTTGGCTTGG-3′; gp100 forward 5′-AGTTCCAGGGACCACAGATG-3′ and reverse 5′-CCAGGCAT GATAAGCTGGGT-3′; GAPDH forward 5′-CCGTCAAGGCTGAGAA CGGG-3′ and reverse 5′-GCCATGCCAGTGAGCTTCCC-3′. The qPCR was performed using PowerUp™ SYBR™ Green Master Mix (Thermo Fisher Scientific) with the following primers: ERAP1 forward 5′-CCCGACTTTCAGTCTGGTGCT-3′ and reverse 5′-TC CCAAACCACTGGTGAGCCA-3′; ERAP2 forward 5′-GTGGCTTCA CTTCATCAGGGGT-3′ and reverse 5′-TCCATGGCTCCAGGTGC AAA-3′; 18S rRNA forward 5′-GTGGAGCGATTTGTCTGGTT-3′ and reverse 5′-AACGCCACTTGTCCCTCTAA-3′. Relative expression levels of the selected transcripts were normalized to the control siRNA and the housekeeping gene 18S rRNA and calculated using the $2^{-\Delta\Delta Ct}$ method.

Identification of ERAP1 allelic variants

To identify the expressed ERAP1 alleles the full length ERAP1 construct derived from total RNA of HeLa^{A2+} cells, Ma-Mel-63a, Ma-Mel-86a and UKRV-Mel-15a cells was cloned into pCR 2.1 plasmid via TA cloning Kit (Thermo Fisher Scientific) and subsequently sequenced and analyzed for previously described allelic variants according to Yao et al. [64].

Acknowledgements: We thank Prof. Axel Kramer for his continuous support. The project was supported by grants of the Deutsche Forschungsgemeinschaft to U.S. (SFB-TR36) and Deutsche Krebshilfe (Nr. 106861) to A.P., U.S. and D.S., Berliner Krebsgesellschaft e.V. (Z:SEFF200907) to U.S. and B.D., by AICE FIRE Onlus Emilia Romagna, Cancer Research UK King's Health Partners Centre at King's College London (Development Fund 2018) and KCL-Monash collaboration award 2018 to M.M. We thank the Shared Facility Mass Spectrometry of the Charité for support in acquisition (i. a. and analysis) of the data.

Author contributions: K.T.T., C.C., A.P., M.M., and U.S. conceived and designed the research. K.T.T., C.C., E.T., F.Z., A.P. and M.M. acquired data. P.H. and W.U. provided material. K.T.T., C.C., F.E., D.S., B.D., W.U., M.M., S.H., J.L. and U.S. analyzed and interpreted data. K.T.T., C.C., A.P., M.M. and U.S. wrote the manuscript.

Conflict of interest: The authors declare no commercial or financial conflict of interest.

References

1 **Rosenberg, S. A. and Restifo, N. P.**, Adoptive cell transfer as personalized immunotherapy for human cancer. *Science* 2015. **348**: 62–68.

2 **Coulie, P. G., Van den Eynde, B. J., van der Bruggen, P. and Boon, T.**, Tumour antigens recognized by T lymphocytes: at the core of cancer immunotherapy. *Nat. Rev. Cancer* 2014. **14**: 135–146.

3 **Ritz, D., Gloger, A., Weide, B., Garbe, C., Neri, D. and Fugmann, T.**, High-sensitivity HLA class I peptidome analysis enables a precise definition of peptide motifs and the identification of peptides from cell lines and patients' sera. *Proteomics* 2016. **16**: 1570–1580.

4 **Liepe, J., Marino, F., Sidney, J., Jeko, A., Bunting, D. E., Sette, A., Kloetzel, P. M. et al.**, A large fraction of HLA class I ligands are proteasome-generated spliced peptides. *Science* 2016. **354**: 354–358.

5 **Mishto, M. and Liepe, J.**, Post-translational peptide splicing and T cell responses. *Trends Immunol.* 2017. **38**: 904–915.

6 **Strehl, B., Seifert, U., Kruger, E., Heink, S., Kuckelkorn, U. and Kloetzel, P. M.**, Interferon-gamma, the functional plasticity of the ubiquitin-proteasome system, and MHC class I antigen processing. *Immunol. Rev.* 2005. **207**: 19–30.

7 **Guillaume, B., Chapiro, J., Stroobant, V., Colau, D., Van Holle, B., Parvizi, G., Bousquet-Dubouch, M. P. et al.**, Two abundant proteasome subtypes that uniquely process some antigens presented by HLA class I molecules. *Proc. Natl. Acad. Sci. U. S. A.* 2010. **107**: 18599–18604.

8 **Zanker, D., Waithman, J., Yewdell, J. W. and Chen, W.**, Mixed proteasomes function to increase viral peptide diversity and broaden antiviral CD8$^+$ T cell responses. *J. Immunol.* 2013. **191**: 52–59.

9 **Klare, N., Seeger, M., Janek, K., Jungblut, P. R. and Dahlmann, B.**, Intermediate-type 20 S proteasomes in HeLa cells: "asymmetric" subunit composition, diversity, and adaptation. *J. Mol. Biol.* 2007. **373**: 1–10.

10 **Mishto, M., Liepe, J., Textoris-Taube, K., Keller, C., Henklein, P., Weberruss, M., Dahlmann, B. et al.**, Proteasome isoforms exhibit only quantitative differences in cleavage and epitope generation. *Eur. J. Immunol.* 2014. **44**: 3508–3521.

11 **Kincaid, E. Z., Che, J. W., York, I., Escobar, H., Reyes-Vargas, E., Delgado, J. C., Welsh, R. M. et al.**, Mice completely lacking immunoproteasomes show major changes in antigen presentation. *Nat. Immunol.* 2011. **13**: 129–135.

12 **Chapiro, J., Claverol, S., Piette, F., Ma, W., Stroobant, V., Guillaume, B., Gairin, J. E. et al.**, Destructive cleavage of antigenic peptides either by the immunoproteasome or by the standard proteasome results in differential antigen presentation. *J. Immunol.* 2006. **176**: 1053–1061.

13 **Guillaume, B., Stroobant, V., Bousquet-Dubouch, M. P., Colau, D., Chapiro, J., Parmentier, N., Dalet, A. et al.**, Analysis of the processing of seven human tumor antigens by intermediate proteasomes. *J. Immunol.* 2012. **189**: 3538–3547.

14 **Kuckelkorn, U., Stubler, S., Textoris-Taube, K., Killian, C., Niewienda, A., Henklein, P., Janek, K. et al**, Proteolytic dynamics of human 20S thymoproteasome. *J. Biol. Chem.* 2019. **294**: 7740–7754.

15 **Liepe, J., Holzhutter, H. G., Bellavista, E., Kloetzel, P. M., Stumpf, M. P. and Mishto, M.**, Quantitative time-resolved analysis reveals intricate, differential regulation of standard- and immuno-proteasomes. *Elife* 2015.**4**.

16 **Seifert, U., Maranon, C., Shmueli, A., Desoutter, J. F., Wesoloski, L., Janek, K., Henklein, P. et al.**, An essential role for tripeptidyl peptidase in the generation of an MHC class I epitope. *Nat. Immunol.* 2003. **4**: 375–379.

17 **Saveanu, L., Carroll, O., Lindo, V., Del Val, M., Lopez, D., Lepelletier, Y., Greer, F. et al.**, Concerted peptide trimming by human ERAP1 and ERAP2 aminopeptidase complexes in the endoplasmic reticulum. *Nat. Immunol.* 2005. **6**: 689–697.

18 **Tanioka, T., Hattori, A., Masuda, S., Nomura, Y., Nakayama, H., Mizutani, S. and Tsujimoto, M.**, Human leukocyte-derived arginine aminopeptidase. The third member of the oxytocinase subfamily of aminopeptidases. *J. Biol. Chem.* 2003. **278**: 32275–32283.

19 **Cifaldi, L., Romania, P., Lorenzi, S., Locatelli, F. and Fruci, D.**, Role of endoplasmic reticulum aminopeptidases in health and disease: from infection to cancer. *Int. J. Mol. Sci.* 2012. **13**: 8338–8352.

20 **Fruci, D., Ferracuti, S., Limongi, M. Z., Cunsolo, V., Giorda, E., Fraioli, R., Sibilio, L. et al.**, Expression of endoplasmic reticulum aminopeptidases in EBV-B cell lines from healthy donors and in leukemia/lymphoma, carcinoma, and melanoma cell lines. *J. Immunol.* 2006. **176**: 4869–4879.

21 **Stoehr, C. G., Buettner-Herold, M., Kamphausen, E., Bertz, S., Hartmann, A. and Seliger, B.**, Comparative expression profiling for human endoplasmic reticulum-resident aminopeptidases 1 and 2 in normal kidney versus distinct renal cell carcinoma subtypes. *Int. J. Clin. Exp. Pathol.* 2013. **6**: 998–1008.

22 **York, I. A., Brehm, M. A., Zendzian, S., Towne, C. F. and Rock, K. L.**, Endoplasmic reticulum aminopeptidase 1 (ERAP1) trims MHC class I-presented peptides in vivo and plays an important role in immunodominance. *Proc. Natl. Acad. Sci. U. S. A.* 2006. **103**: 9202–9207.

23 **James, E., Bailey, I., Sugiyarto, G. and Elliott, T.**, Induction of protective antitumor immunity through attenuation of ERAAP function. *J. Immunol.* 2013. **190**: 5839–5846.

24 **Keller, M., Ebstein, F., Burger, E., Textoris-Taube, K., Gorny, X., Urban, S., Zhao, F. et al.** The proteasome immunosubunits, PA28 and ER-aminopeptidase 1 protect melanoma cells from efficient MART-126-35 -specific T-cell recognition. *Eur. J. Immunol.* 2015. **45**: 3257–3268.

25 **Mpakali, A., Maben, Z., Stern, L. J. and Stratikos, E.**, Molecular pathways for antigenic peptide generation by ER aminopeptidase 1. *Mol. Immunol.* 2019. **113**: 50–57.

26 **Stratikos, E., Stamogiannos, A., Zervoudi, E. and Fruci, D.**, A role for naturally occurring alleles of endoplasmic reticulum aminopeptidases in tumor immunity and cancer pre-disposition. *Front. Oncol.* 2014. **4**: 363.

27 **Evnouchidou, I., Weimershaus, M., Saveanu, L. and van Endert, P.**, ERAP1-ERAP2 dimerization increases peptide-trimming efficiency. *J. Immunol.* 2014. **193**: 901–908.

28 **Chen, H., Li, L., Weimershaus, M., Evnouchidou, I., van Endert, P. and Bouvier, M.**, ERAP1-ERAP2 dimers trim MHC I-bound precursor peptides; implications for understanding peptide editing. *Sci. Rep.* 2016. **6**: 28902.

29 **Blees, A., Januliene, D., Hofmann, T., Koller, N., Schmidt, C., Trowitzsch, S., Moeller, A. et al.**, Structure of the human MHC-I peptide-loading complex. *Nature* 2017. **551**: 525–528.

30 **Blum, J. S., Wearsch, P. A. and Cresswell, P.**, Pathways of antigen processing. *Annu. Rev. Immunol.* 2013. **31**: 443–473.

31 **Kawakami, Y., Eliyahu, S., Jennings, C., Sakaguchi, K., Kang, X., Southwood, S., Robbins, P. F. et al.**, Recognition of multiple epitopes in the human melanoma antigen gp100 by tumor-infiltrating T lymphocytes associated with in vivo tumor regression. *J. Immunol.* 1995. **154**: 3961–3968.

32 **Smith, F. O., Downey, S. G., Klapper, J. A., Yang, J. C., Sherry, R. M., Royal, R. E., Kammula, U. S. et al.**, Treatment of metastatic melanoma using interleukin-2 alone or in conjunction with vaccines. *Clin. Cancer Res.* 2008. **14**: 5610–5618.

33 **Rosenberg, S. A., Yang, J. C., Schwartzentruber, D. J., Hwu, P., Marincola, F. M., Topalian, S. L., Restifo, N. P. et al.**, Immunologic and therapeutic evaluation of a synthetic peptide vaccine for the treatment of patients with metastatic melanoma. *Nat. Med.* 1998. **4**: 321–327.

34 **Schwartzentruber, D. J., Lawson, D. H., Richards, J. M., Conry, R. M., Miller, D. M., Treisman, J., Gailani, F. et al.**, gp100 peptide vaccine and interleukin-2 in patients with advanced melanoma. *N. Engl. J. Med.* 2011. **364**: 2119–2127.

35 **Textoris-Taube, K., Keller, C., Liepe, J., Henklein, P., Sidney, J., Sette, A., Kloetzel, P. M. et al.**, The T210M substitution in the HLA-a*02:01 gp100 epitope strongly affects overall proteasomal cleavage site usage and antigen processing. *J. Biol. Chem.* 2015. **290**: 30417–30428.

36 **Bakker, A. B., Schreurs, M. W., Tafazzul, G., de Boer, A. J., Kawakami, Y., Adema, G. J. and Figdor, C. G.**, Identification of a novel peptide derived from the melanocyte-specific gp100 antigen as the dominant epitope recognized by an HLA-A2.1-restricted anti-melanoma CTL line. *Int. J. Cancer* 1995. **62**: 97–102.

37 **Mishto, M., Goede, A., Taube, K. T., Keller, C., Janek, K., Henklein, P., Niewienda, A. et al.**, Driving forces of proteasome-catalyzed peptide splicing in yeast and humans. *Mol. Cell. Proteomics* 2012. **11**: 1008–1023.

38 **Dalet, A., Robbins, P. F., Stroobant, V., Vigneron, N., Li, Y. F., El-Gamil, M., Hanada, K. I. et al.**, An antigenic peptide produced by reverse splicing and double asparagine deamidation. *Proc. Natl. Acad. Sci. U. S. A.* 2011. **108**: E323-E331.

39 **Dalet, A., Stroobant, V., Vigneron, N. and Van den Eynde, B. J.**, Differences in the production of spliced antigenic peptides by the standard proteasome and the immunoproteasome. *Eur. J. Immunol.* 2011. **41**: 39–46.

40 **Ebstein, F., Textoris-Taube, K., Keller, C., Golnik, R., Vigneron, N., Van den Eynde, B. J., Schuler-Thurner, B. et al.**, Proteasomes generate spliced epitopes by two different mechanisms and as efficiently as non-spliced epitopes. *Sci. Rep.* 2016. **6**: 24032.

41 **Michaux, A., Larrieu, P., Stroobant, V., Fonteneau, J. F., Jotereau, F., Van den Eynde, B. J., Moreau-Aubry, A. et al.**, A spliced antigenic peptide comprising a single spliced amino acid is produced in the proteasome by reverse splicing of a longer peptide fragment followed by trimming. *J. Immunol.* 2014. **192**: 1962–1971.

42 **Platteel, A. C., Mishto, M., Textoris-Taube, K., Keller, C., Liepe, J., Busch, D. H., Kloetzel, P. M. et al.**, CD8 T cells of Listeria monocytogenes-infected mice recognize both linear and spliced proteasome products. *Eur. J. Immunol.* 2016. **46**: 1109–1118.

43 **Platteel, A. C. M., Liepe, J., Textoris-Taube, K., Keller, C., Henklein, P., Schalkwijk, H. H., Cardoso, R. et al.**, Multi-level strategy for identifying proteasome-catalyzed spliced epitopes targeted by $CD8^+$ T cells during bacterial infection. *Cell Rep.* 2017. **20**: 1242–1253.

44 **Vigneron, N., Stroobant, V., Chapiro, J., Ooms, A., Degiovanni, G., Morel, S., van der Bruggen, P. et al.**, An antigenic peptide produced by peptide splicing in the proteasome. *Science* 2004. **304**: 587–590.

45 **Warren, E. H., Vigneron, N. J., Gavin, M. A., Coulie, P. G., Stroobant, V., Dalet, A., Tykodi, S. S. et al.**, An antigen produced by splicing of

noncontiguous peptides in the reverse order. *Science* 2006. **313**: 1444–1447.

46 **Tenzer, S., Wee, E., Burgevin, A., Stewart-Jones, G., Friis, L., Lamberth, K., Chang, C. H. et al.**, Antigen processing influences HIV-specific cytotoxic T lymphocyte immunodominance. *Nat. Immunol.* 2009. **10**: 636–646.

47 **Deol, P., Zaiss, D. M., Monaco, J. J. and Sijts, A. J.**, Rates of processing determine the immunogenicity of immunoproteasome-generated epitopes. *J. Immunol.* 2007. **178**: 7557–7562.

48 **Mehta, A. M., Jordanova, E. S., van Wezel, T., Uh, H. W., Corver, W. E., Kwappenberg, K. M., Verduijn, W. et al.**, Genetic variation of antigen processing machinery components and association with cervical carcinoma. *Genes Chromosomes Cancer* 2007. **46**: 577–586.

49 **Yao, Y., Wisniewski, A., Ma, Q., Kowal, A., Porebska, I., Pawelczyk, K., Yu, J. et al.**, Single nucleotide polymorphisms of the ERAP1 gene and risk of NSCLC: a comparison of genetically distant populations, Chinese and Caucasian. *Arch. Immunol. Ther. Exp. (Warsz)* 2016. **64**: 117–122.

50 **Reeves, E., Elliott, T., Edwards, C. J. and James, E.**, Both rare and common ERAP1 allotypes have distinct functionality defined by polymorphic context and are important in AS association. *Proc. Natl. Acad. Sci. U. S. A.* 2017. **114**: E1575-E1576.

51 **Hodi, F. S., O'Day, S. J., McDermott, D. F., Weber, R. W., Sosman, J. A., Haanen, J. B., Gonzalez, R. et al.**, Improved survival with ipilimumab in patients with metastatic melanoma. *N. Engl. J. Med.* 2010. **363**: 711–723.

52 **McDermott, D., Haanen, J., Chen, T. T., Lorigan, P., O'Day, S. and Investigators, M. D. X.**, Efficacy and safety of ipilimumab in metastatic melanoma patients surviving more than 2 years following treatment in a phase III trial (MDX010-20). *Ann. Oncol.* 2013. **24**: 2694–2698.

53 **Mehta, A. M., Osse, M., Kolkman-Uljee, S., Fleuren, G. J. and Jordanova, E. S.**, Molecular backgrounds of ERAP1 downregulation in cervical carcinoma. *Anal. Cell. Pathol. (Amst)* 2015. **2015**: 367837.

54 **Vigneron, N., Ferrari, V., Van den Eynde, B. J., Cresswell, P. and Leonhardt, R. M.**, Cytosolic processing governs TAP-independent presentation of a critical melanoma antigen. *J. Immunol.* 2018. **201**: 1875–1888.

55 **Ugurel, S., Thirumaran, R. K., Bloethner, S., Gast, A., Sucker, A., Mueller-Berghaus, J., Rittgen, W. et al.**, B-RAF and N-RAS mutations are preserved during short time in vitro propagation and differentially impact prognosis. *PLoS One* 2007. **2**: e236.

56 **Kuckelkorn, U., Frentzel, S., Kraft, R., Kostka, S., Groettrup, M. and Kloetzel, P. M.**, Incorporation of major histocompatibility complex–encoded subunits LMP2 and LMP7 changes the quality of the 20S proteasome polypeptide processing products independent of interferon-gamma. *Eur. J. Immunol.* 1995. **25**: 2605–2611.

57 **Urban, S., Textoris-Taube, K., Reimann, B., Janek, K., Dannenberg, T., Ebstein, F., Seifert, C. et al.**, The efficiency of human cytomegalovirus pp65(495-503) CD8+ T cell epitope generation is determined by the balanced activities of cytosolic and endoplasmic reticulum-resident peptidases. *J. Immunol.* 2012. **189**: 529–538.

58 **Ebstein, F., Lange, N., Urban, S., Seifert, U., Kruger, E. and Kloetzel, P. M.**, Maturation of human dendritic cells is accompanied by functional remodelling of the ubiquitin-proteasome system. *Int. J. Biochem. Cell Biol.* 2009. **41**: 1205–1215.

59 **Oh, I. S., Textoris-Taube, K., Sung, P. S., Kang, W., Gorny, X., Kahne, T., Hong, S. H. et al.**, Immunoproteasome induction is suppressed in hepatitis C virus-infected cells in a protein kinase R-dependent manner. *Exp. Mol. Med.* 2016. **48**: e270.

60 **Gohlke, S., Kloss, A., Tsokos, M., Textoris-Taube, K., Keller, C., Kloetzel, P. M. and Dahlmann, B.**, Adult human liver contains intermediate-type proteasomes with different enzymatic properties. *Ann. Hepatol.* 2014. **13**: 429–438.

61 **Liepe, J., Mishto, M., Textoris-Taube, K., Janek, K., Keller, C., Henklein, P., Kloetzel, P. M. et al.**, The 20S proteasome splicing activity discovered by SpliceMet. *PLoS Comput. Biol.* 2010. **6**: e1000830.

62 **Cox, J., Hein, M. Y., Luber, C. A., Paron, I., Nagaraj, N. and Mann, M.**, Accurate proteome-wide label-free quantification by delayed normalization and maximal peptide ratio extraction, termed MaxLFQ. *Mol. Cell. Proteomics* 2014. **13**: 2513–2526.

63 **Kieback, E., Charo, J., Sommermeyer, D., Blankenstein, T. and Uckert, W.**, A safeguard eliminates T cell receptor gene-modified autoreactive T cells after adoptive transfer. *Proc. Natl. Acad. Sci. U. S. A.* 2008. **105**: 623–628.

64 **Yao, Y., Liu, N., Zhou, Z. and Shi, L.**, Influence of ERAP1 and ERAP2 gene polymorphisms on disease susceptibility in different populations. *Hum. Immunol.* 2019. **80**: 325–334.

Abbreviations: **APP**: antigen processing and presentation pathway · **ERAP**: ER-aminopeptidase · **gp100**$_{209\text{-}217/T210M}$: wild type and mutated sequence · **gp100**$_{209\text{-}217/(T210M)}$: mutated sequence · **LMP**: low molecular weight protein · **HeLa^{A2+}**: HeLa cells expressing HLA-A*02:01 · **LC-MS**: liquid-chromatography–mass spectrometry · **MECL-1**: multicatalytic endopeptidase complex like 1 · **MS**: mass spectrometry · **PMEL/Pmel17**: premelanosome protein · **QME**: quantification with minimal effort · **SCS**: site-specific cleavage strength · **TPP2**: tripeptidyl peptidase 2

Full correspondence: Prof. Ulrike Seifert, Friedrich Loeffler Institut für Medizinische Mikrobiologie-Virologie, Universitätsmedizin Greifswald KdöR, Ferdinand-Sauerbruch-Straße, 17475 Greifswald, Germany
e-mail: ulrike.seifert@med.uni-greifswald.de

Present address: Frédéric Ebstein, Institut für Medizinische Biochemie und Molekularbiologie, Universitätsmedizin Greifswald, Greifswald, Germany

Received: 22/1/2019
Revised: 19/8/2019
Accepted: 13/11/2019
Accepted article online: 15/11/2019